

SCHOOL OF MECHANICAL AND AEROSPACE ENGINEERING MA3071 – ENGINEERING EXPERIMENTS (ME)

P3.4 ULTIMATE LOAD OF BEAMS UNDER BENDING

FORMAL REPORT

MECHANICS OF MATERIALS LAB

N3.2-B2-01

NAME: CHIA CHIN ANN CALEB (U2121391K)

LAB GROUP: ME37

FACULTY-IN-CHARGE: DR. LI HUA

DATE OF SUBMISSION: 22nd FEBRUARY 2023

1 ABSTRACT

In this experiment, we aim to determine how aluminium beams of two different cross-sections (C-Shape Beam and Rectangular Beam) will react when they are subjected to a three-point and four-point bending test using a hydraulic press machine respectively. The test will be performed until the aluminium beam reaches the plastic region before we start to unload the force applied. We will then reinforce the C-Shape aluminium beam to overcome the buckling effects by adding more material to further strengthen it.

2 INTRODUCTION

When a load is applied on a beam, it will transfer the load by converting them into internal shear forces and moments. The moments can result in notable tensile and compressive stresses within the beam. Shear stresses may also be important for beams with small span-to-depth ratios.

If only internal moments are acting within a beam element, it is known to be under pure bending. As shown in Figure 1, the central span of a beam under four-point loading is subjected to pure bending. In comparison, a beam subjected to three-point bending will experience both shear forces and moments throughout the span except for the supports as shown in Figure 2. Moreover, the gradient of the shear force at the midpoint experiences a lack of coherence.

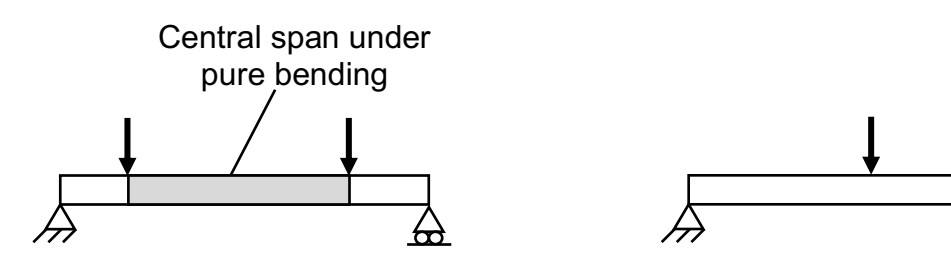


Figure 1. Four-point bending of a beam Figure 2. Three-point bending of a beam

How the beam reacts also depends on its elemental properties. A material's yield stress σ_y is the stress where it transits from elastic to plastic behaviour. The stress-strain relation is linear elastic initially and perfectly plastic after the yield stress is reached as reflected in Figure 3. When a beam experiences a sufficiently large load, the maximum of the normal stress σ_x occurs and the outermost fibres of a cross-

section, reach the yield stress first, and the corresponding moment is known as the moment to first yield M_V .

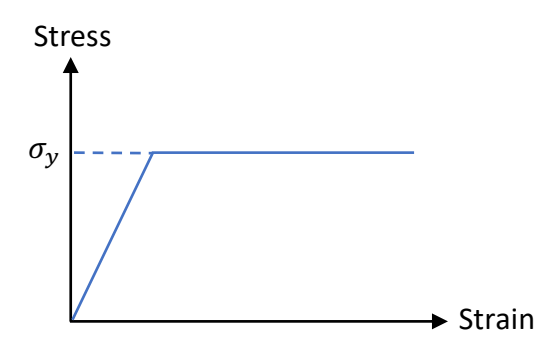


Figure 3. Constitutive elastic-plastic response of a material

In Figure 4, it displays the fundamental concepts for the case of a rectangular beam. The interior region of the cross-section remains elastic, but this elastic core will continue to get smaller if the bending moment increases beyond M_Y . Once the maximum is reached, the entire cross-section may yield and the elastic core may disappear. The corresponding moment is the plastic moment M_P . Designs of beams that consider M_P may be more cost-effective and efficient than those only factoring in M_Y .

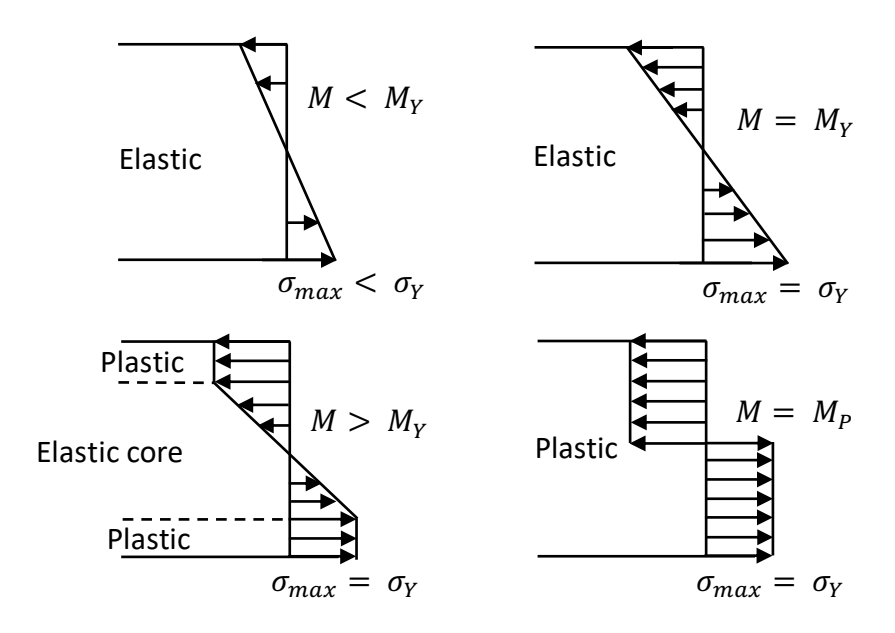


Figure 4. Distributions of normal stress σ_x in a rectangular cross section

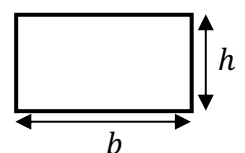
3 OBJECTIVES

- (a) To determine experimentally M_Y and M_P , and hence the shape factor $k = M_P/M_Y$, for beams with rectangular and C-Shape cross-sections subjected to (i) four-point bending, and (ii) three-point bending.
- (b) To determine the residual radii of curvature ρ_r of the rectangular beams, after the maximum load placed on each beam has been completely removed.
- (c) To design and construct reinforcement of the C-Shape beam with the aim of suppressing buckling.
- (d) To compute the theoretical values of M_Y , M_P and k for both the rectangular and C-section beams, and ρ_r and the residual stress distributions for only the rectangular beams. Calculations are to be carried out for the un-reinforced beams.

4 THEORY

Deformations of a prismatic member possessing a plane of symmetry and subjected at its ends will have equal and opposite couples acting in the plane of symmetry. The member will bend due to the couples involved but will stay symmetric with respect to the plane, which is classified as pure bending. Pure bending will result in the beam experiencing compressive stress on the beam's upper region while tension stress on the beam's lower region. The neutral axis that passes through the centroid of the cross-section is the axis that experiences neither compressive nor tension stress.

4.1 THEORETICAL CALCULATIONS OF M_Y , M_P and k FOR RECTANGULAR CROSS-SECTION BEAM



In the elastic regime,

$$\sigma = -\frac{My}{I}$$
, where second moment of area $I = \frac{1}{12}bh^3$

When the outermost fibres reach yield stress σ_y , $y = -\frac{h}{2}$, resulting in,

$$M_Y = \frac{1}{6}bh^3\sigma_y$$

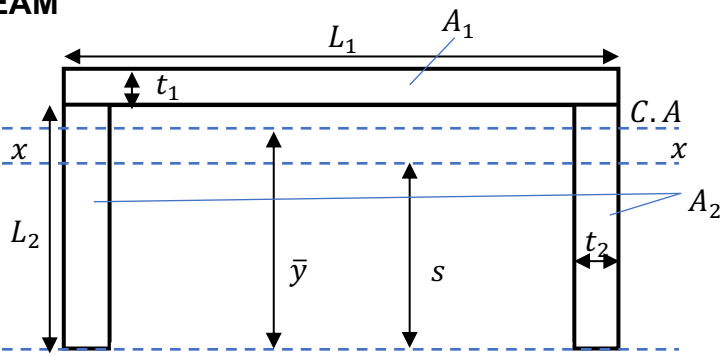
When the beam becomes fully plastic, the neutral axis equally divides the areas above and below the axis, and for this rectangular cross-section, it still remains as the centroidal axis. Therefore,

$$M_P = \frac{1}{4}bh^2\sigma_y$$

The shape function k is thus

$$k = \frac{M_P}{M_Y} = \frac{3}{2}$$

4.2 THEORETICAL CALCULATIONS OF $M_Y,\,M_P\,$ and k FOR C-SHAPE CROSS-SECTION BEAM



For a C-Shape cross-section beam, we will need to first calculate the centroidal axis C.A., which is a distance \bar{y} above the reference axis. This is done by taking area moments about the reference axis.

$$A_1\left(L_2 + \frac{t_1}{2}\right) + 2A_2\left(\frac{L_2}{2}\right) = (A_1 + 2A_2)\bar{y}$$

Next, the second moment of area *I* will be obtained by using the parallel axis theorem.

$$I = I_1 + 2I_2$$

$$I_1 = \frac{1}{12}L_1t_1^3 + (L_1t_1)d_1^2 \qquad I_2 = \frac{1}{12}t_2L_2^3 + (L_2t_2)d_2^2$$

where d_1 and d_2 are the respective distances of the centroids of A_1 and A_2 from the centroidal axis.

In this elastic regime, and under pure bending with the absence of axial loads, the C.A. always coincides with the neutral axis (N.A.). Therefore when the outermost (bottom) fibres first reach yield stress σ_y , $y=-\bar{y}$.

$$M_Y = \frac{\sigma_y I}{\bar{y}}$$

When the C-Shape cross-section beam becomes fully plastic, the "new" N.A., denoted by x-x, divides the cross-section into two equal areas above and below x-x. Therefore

$$M_P = \left(\sigma_y A_1\right) \left(L_2 - s + \left(\frac{t_1}{2}\right)\right) + 2\left(\sigma_y \left(t_2 (L_2 - s)\right)\right) \left(\frac{L_2 - s}{2}\right) + 2\left(\sigma_y (t_2 s) \left(\frac{s}{2}\right)\right)$$

The shape factor k can be determined as M_P and M_Y have been known.

4.3 THEORETICAL CALCULATIONS OF RESIDUAL STRESS DISTRIBUTION FOR RECTANGULAR CROSS-SECTION BEAM

A member made of an elastoplastic material will deform obeying Hooke's law as long as the normal stress σ_x does not surpass the yield strength σ_y . Member will become plastic once $\sigma > \sigma_y$. Hence, the surface of the beam which is furthest away from the neutral axis will become plastic first due to the larger σ experienced. When bending is sufficiently large, the plastic zones will form in the member made of elastoplastic material. When the bending has dropped to zero, the resultant stress at a point will not be zero due to residual stresses. As shown in Figure 5, residual stresses that remain in the various parts of the beam are derived by applying the principle of superposition.

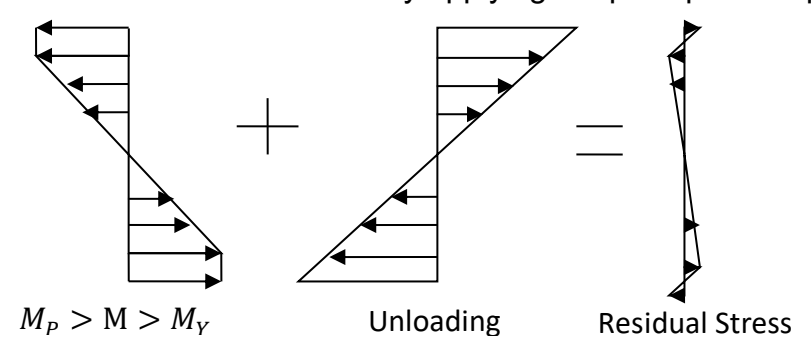


Figure 5. Determination of residual stress using superposition

The "fictitious" maximum stress σ_m is as follows

$$\sigma_m = \frac{M(\frac{h}{2})}{I} = \frac{M(\frac{h}{2})}{\frac{1}{12}bh^3} = \frac{6M}{bh^2}$$

5 EXPERIMENTAL DETAILS

5.1 EQUIPMENT LIST

- (1) Shimadzu AGX 100kN Materials Tester
- (2) Three points testing fixture
- (3) Four points testing fixture

5.2 PROCEDURES

- (1) Fix the appropriate load head for 3 or 4-point measurement.
- (2) Orientate the workpiece equally onto the supports.
- (3) Lower the load head manually using the controller till it is firmly held by the test rig.
- (4) Calibrate and zero the displacement measurement sensor before allowing the load to be applied automatically using the *TRAPEZIUM X* software.
- (5) Record a stress vs strain graph using the TRAPEZIUM X software.
- (6) Once ultimate tensile stress is displayed on the graph, stop applying the load on the workpiece.
- (7) Using the controller, manually raise the load head and remove the workpiece.
- (8) Repeat the experiment from steps 1 to 7 for the different beams as well as for the different point loadings.

6 RESULTS

6.1 TECHNICAL DATA

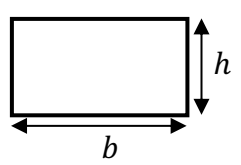
MATERIAL PROPERTIES

Based on the tensile test for Aluminium 6061, we have obtained the following results: $\sigma_v = 220 \text{MPa} \text{ and } E = 68 \text{GPa}$

RECTANGULAR CROSS-SECTION BEAM

$$b = 50.9mm = 0.0509m$$

$$h = 12.7mm = 0.0127m$$

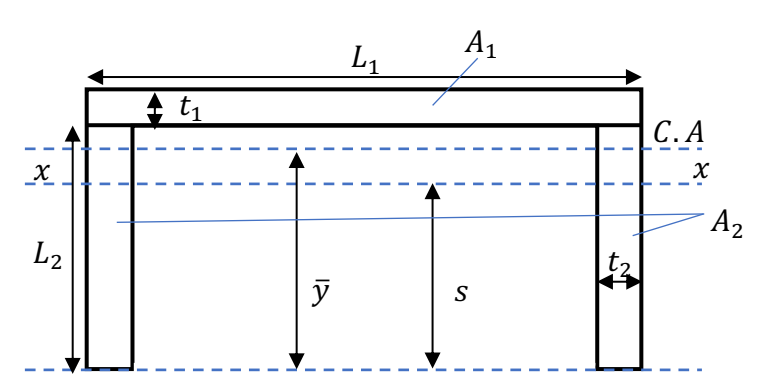


C-SHAPE CROSS-SECTION BEAM

$$L_1 = 78.4mm = 0.0784m$$

$$L_2 = 24.5mm = 0.0245m$$

$$t_1 = t_2 = 1mm = 0.001m$$



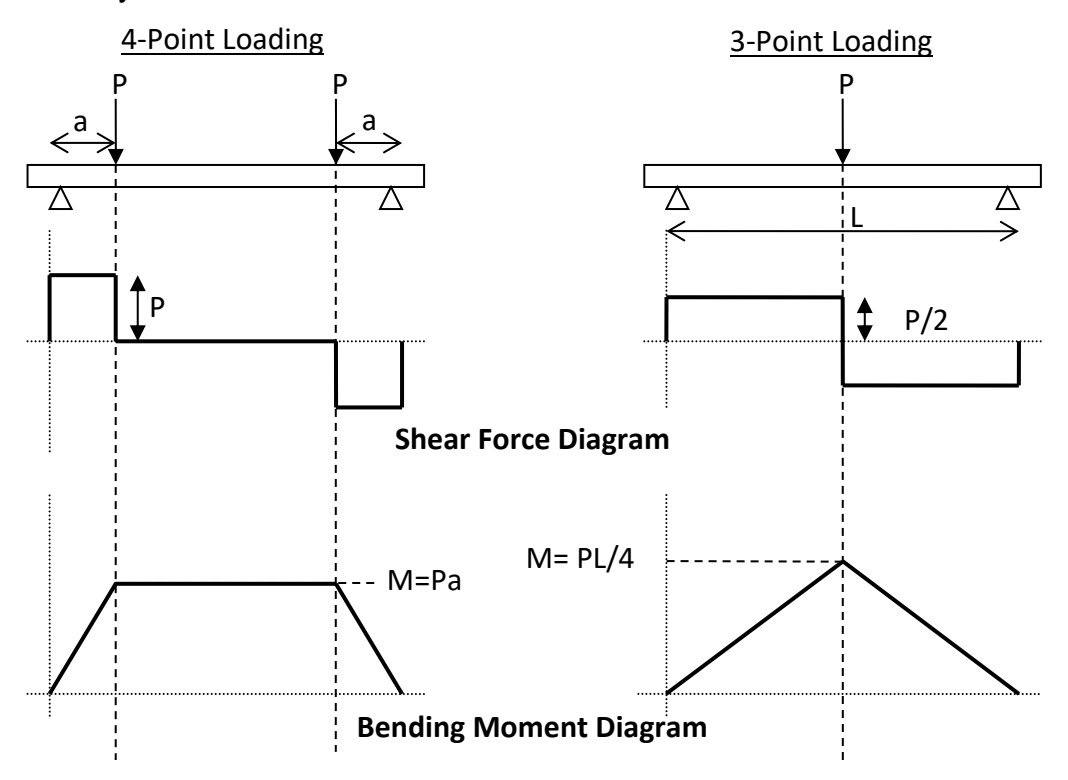
6.2 EXPERIMENTAL RESULTS

Graphs obtained from the experiment are shown in Appendix.

From the graphs, the following experimental results were obtained:

	Rectangular		C-Shape		Reinforced C-Shape	
Loading	3-Point	4-Point	3-Point	4-Point	3-Point	4-Point
P_Y (kN)	2.082	1.497	0.501	0.414	0.806	0.607
P_P (kN)	3.023	2.267	0.795	0.665	1.245	0.920

Under loading, the force acting on the beam can be used to determine the shear force and bending moment diagram. The values of M_Y and M_P can hence be determined experimentally.



where a = 0.202m and L = 0.7m.

Hence the experimental results are as follows:

	Rectangular		C-Shape		Reinforced C-Shape	
Loading	3-Point	4-Point	3-Point	4-Point	3-Point	4-Point
M_Y (kNm)	0.364	0.302	0.088	0.084	0.141	0.106
M_P (kNm)	0.529	0.458	0.139	0.134	0.218	0.161
$k = \frac{M_P}{M_Y}$	1.45	1.51	1.59	1.61	1.55	1.52
ho (m)	1.394	1.765	-	-	-	-

6.3 THEORETICAL CALCULATIONS

Rectangular Shape Beam

\(\(\) \(200 406 P			
Yield Stress	$\sigma_y = 220 \times 10^6 Pa$			
Neutral Axis/	$\bar{y} = n = \frac{0.0127}{2} = 0.00635m$			
Centroidal Axis	$y = n = \frac{1}{2} = 0.00635m$			
Second Moment	$I = \frac{1}{(0.0500)(0.0127)^3} = 0.000 \times 10^{-9} \text{m}^4$			
of Inertia	$I = \frac{1}{12}(0.0509)(0.0127)^3 = 8.689 \times 10^{-9} m^4$			
Yielding Moment	$M_Y = \frac{1}{6}(0.0509)(0.0127)^2(220 \times 10^6) = 301.021 \text{Nm}$			
Ultimate Moment	$M_P = \frac{1}{4}(0.0509)(0.0127)^2(220 \times 10^6) = 451.531 Nm$			
Shape Function	$k = \frac{M_P}{M_Y} = 1.5$			
	$M_P > M > M_Y$, therefore M = $\frac{301.021+451.531}{2}$ = 376.276 Nm			
	$M = \frac{3}{2}M_Y \left(1 - \frac{Y_Y^2}{3\bar{y}^2}\right); Y_Y = 4.490 \times 10^{-3}m$			
Posidual Padiua	Section modulus, $\frac{I}{\overline{y}} = 1.368 \times 10^{-6} m^3$			
Residual Radius Of Curvature	$\sigma_a = \frac{M\bar{y}}{I} = 274.986 MPa$			
	$\sigma_{residual} = \sigma_y - \sigma_a = -54.986 MPa$			
	$\varepsilon_{residual} = \frac{\sigma_{residual}}{E} = -8.042 \times 10^{-4}$			
	$\rho_{residual} = -\frac{y}{\varepsilon_{residual}} = 5.583m$			
Residual Stress	$M_P > M > M_Y$, therefore M = $\frac{301.021+451.531}{2}$ = 376.276 Nm			
Distributions	6(376.276)			
בווטווטמווטווס	$\sigma_m = \frac{6(376.276)}{(0.0509)(0.0127)^2} = 275.000 MPa$			

Unreinforced C-Shape Cross-Section Beam

Yield Stress	$\sigma_y = 220 \times 10^6 Pa$
Neutral Axis	Let a be the distance above the horizontal length of A_1
	$2L_1t_2 + L_1a = (1-a)L_1$
	a = 0.1875 mm
	s = 24.5 + 0.1875 = 24.6875 mm = 0.0246875 m
0 1 11 14 1	$\bar{y} = \frac{(78.4 \times 10^{-6}) \left(0.0245 + \frac{0.001}{2}\right) + 2(25.4 \times 10^{-6}) \left(\frac{0.0245}{2}\right)}{(5.0045 + 0.001) \left(0.0245 + \frac{0.001}{2}\right)}$
Centroidal Axis	$y = {(78.4 \times 10^{-6}) + 2(25.4 \times 10^{-6})}$
	= 0.0200 m
Second Moment	$\bar{y} = \frac{(78.4 \times 10^{-6}) \left(0.0245 + \frac{0.001}{2}\right) + 2(25.4 \times 10^{-6}) \left(\frac{0.0245}{2}\right)}{(25.4 \times 10^{-6}) \left(\frac{0.0245}{2}\right)}$
of Inertia	$\bar{y} = \frac{27}{(78.4 \times 10^{-6}) + 2(25.4 \times 10^{-6})}$

	= 0.0200 m
	$d_1 = \frac{0.001}{2} + 0.0245 - \bar{y} = 0.005m$
	$d_2 = \frac{0.0245}{2} - (0.0245 - \bar{y}) = 0.00775m$
	$I_1 = \frac{1}{12}(0.0784)(0.001)^3 + (0.0784)(0.001)(0.005)^2$
	$= 1.967 \times 10^{-9} m^4$
	$I_2 = \frac{1}{12}(0.001)(0.0245)^3 + (0.0245)(0.001)(0.00775)^2$
	$= 2.697 \times 10^{-9} m^4$
	$I = I_1 + 2I_2 = 7.361 \times 10^{-9} m^4$
Yielding Moment	$M_Y = \frac{(220 \times 10^6)(7.361 \times 10^{-9})}{0.0200 m^4} = 80.967 Nm$
Ultimate Moment	$M_P = \left(\sigma_y A_1\right) \left(L_2 - s + \left(\frac{t_1}{2}\right)\right) + 2\left(\sigma_y \left(t_2 (L_2 - s)\right)\right) \left(\frac{L_2 - s}{2}\right)$
	$+2(\sigma_y(t_2s)\left(\frac{s}{2}\right)$
	= 134.076 + 0.303 + 5.693 = 140.07 Nm
Shape Function	$k = \frac{M_P}{M_Y} = 1.730$

7 DISCUSSIONS

1) What are the main error sources for your testing data?

One source of error is that the load head is not placed perpendicular to the longitudinal axis of the beam. This will result in the beam experiencing shear force and not having "true" pure bending. A possible solution is to have guides so as to ensure that the beam is always accurately positioned as it bends. Another source of error could be friction at the contact points between the beam and the load head. This will cause some of the load applied to not be channelled directly to the beam but is used to overcome the friction of the contacting surface. To reduce the friction, we can consider mildly lubricating the surface to ensure that not too much of the force applied is lost due to friction but we cannot fully eliminate the friction otherwise the beam will slip and not be able to experience the bending effect.

2) What does the shape factor mean? For beams with the same cross-section shape, will the shape factor you obtained from 3-point bending differ from the one in 4point bending? The shape factor is an indicator of how much more loading can the beam sustain after it has yielded but before a plastic hinge is formed. The shape factor for beams with the same cross-section shape should not differ because the shape factor uniquely characterizes the shape regardless of it being a 3-point or 4-point bending. However, in the data obtained from our experiment, the 3-point and 4-point bending yielded differing shape factor values. This could be due to the possible errors mentioned above.

3) What is the logical thinking behind your design of reinforcement of the C-shape beams?

Photos of the reinforcement of the C-shape beams to suppress buckling has been appended in the Appendix. We decided to add material to strengthen where the load was acting on and kept the rivets fixed as low as possible to reduce the shear forces they will face. We also added an additional layer of material on each side of the walls of the C-shape beam to reduce the chances of it buckling. From our results, we managed to strengthen the beam by 56.6% for the 3-point loading. While for the 4-point bending, the strength improved by 38.3% but the reinforcement failed due to one of the rivets giving way. It was observed that a good design of reinforced beams should not have too many rivets at the sides of the metal near to the loading point as this will greatly weaken the strength of the metal on the sides and also add on more mass. Furthermore, we also took note not to add to much material when reinforcing to ensure that the mass of the beams was kept as low as possible. The masses of our 3-point and 4-point reinforced C-shape beams are 385g and 415g respectively.

4) What is the definition of "pure bending"?

If a beam is loaded in a manner such that the shear forces are zero on any crosssection perpendicular to the longitudinal axis of the beam, and therefore it is subjected to only constant bending moment, then the beam is experiencing pure bending.

8 CONCLUSION

In an overview, the primary objectives of the experiment have been achieved. However, there are limitations towards the accuracy of the measurements in the experiments, resulting in the various errors shown in the results. A better setup and choice of equipment for these experiments could be implemented to minimize potential errors and attain much higher accuracy results.

9 REFERENCES

- (1) Beer E. F. P., Johnston, Jr. E. R., DeWolf J. T., Mazurek D. F. (2011). Mechanics of Materials. McGraw Hill.
- (2) Nanyang Technological University. (2023). P3.4 Ultimate Load Of Beams Under Bending.

10 APPENDIX

10.1 RECTANGULAR CROSS-SECTION BEAM

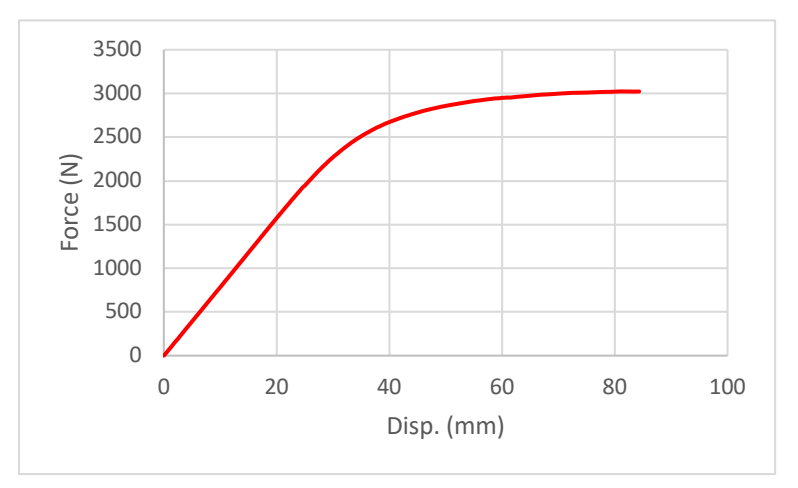


Figure 6. 3-Point Bending Test on Rectangular Cross-Section Beam

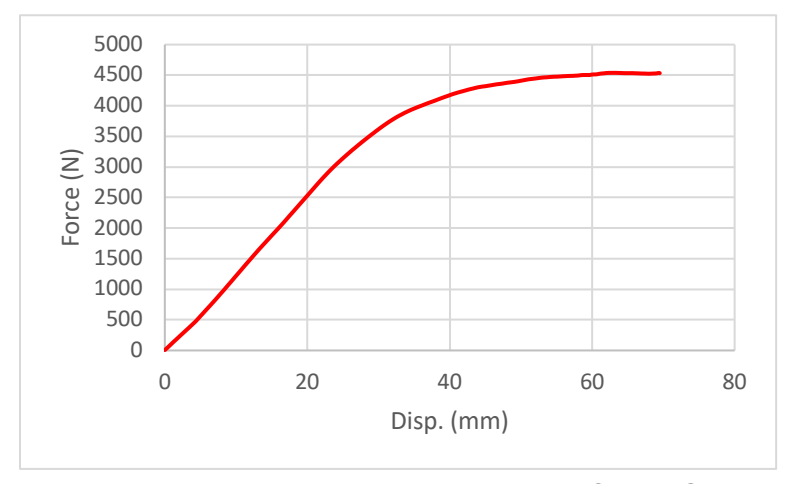


Figure 7. 4-Point Bending Test on Rectangular Cross-Section Beam

10.2 UNREINFORCED C-SHAPE CROSS-SECTION BEAM

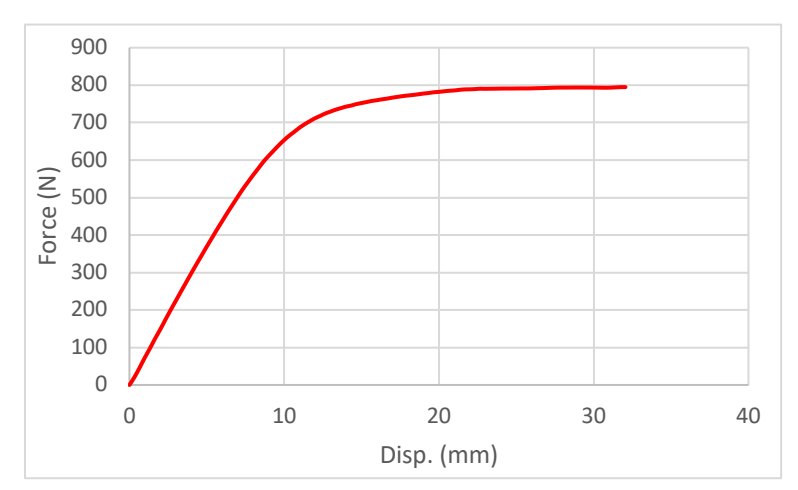


Figure 8. 3-Point Bending Test on Unreinforced C-Shape Cross-Section Beam

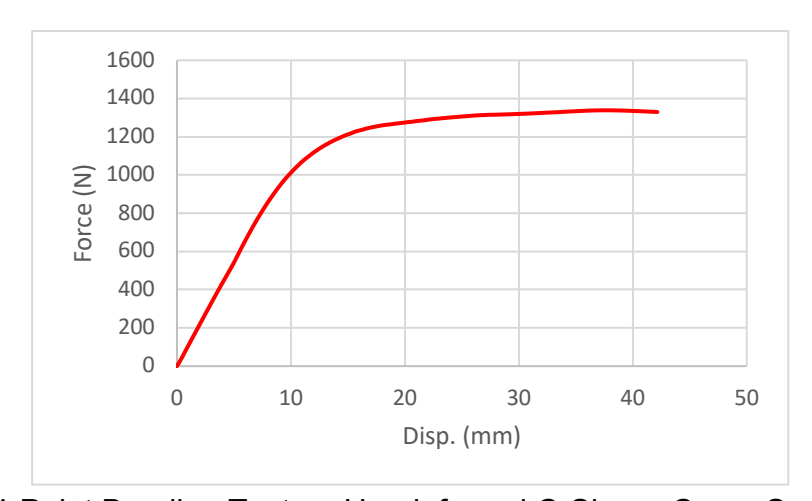


Figure 9. 4-Point Bending Test on Unreinforced C-Shape Cross-Section Beam

10.3 REINFORCED C-SHAPE CROSS-SECTION BEAM

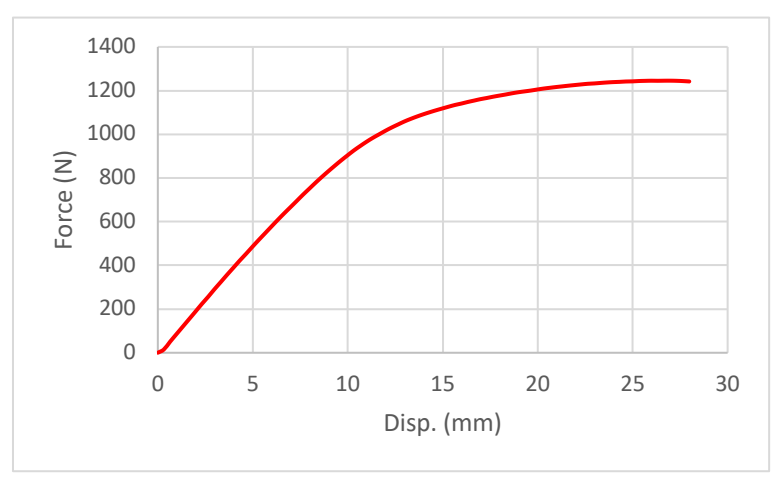


Figure 10. 3-Point Bending Test on Reinforced C-Shape Cross-Section Beam

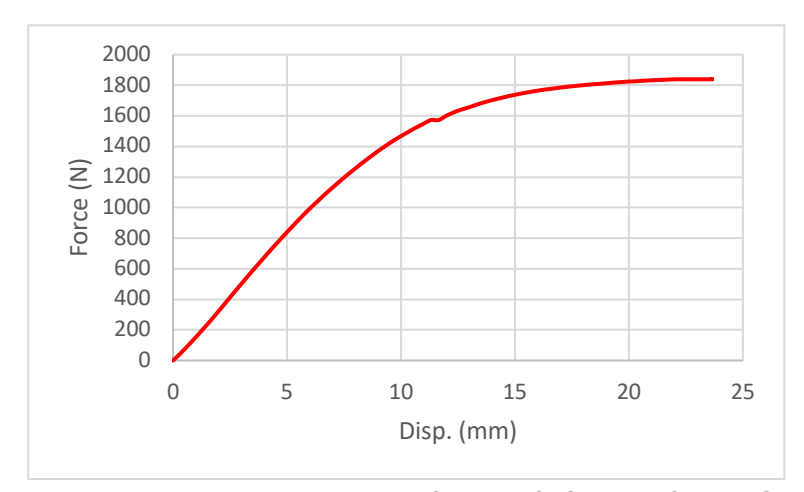


Figure 11. 4-Point Bending Test on Reinforced C-Shape Cross-Section Beam

10.4 PHOTOS OF UNREINFORCED AND REINFORCED C-SHAPE CROSS-SECTION BEAMS



Figure 12. 3-Point Bending Test on Rectangular and Unreinforced C-Shape Cross-Section Beam



Figure 13. 4-Point Bending Test on Rectangular and Unreinforced C-Shape Cross-Section Beam



Figure 14. Design for Reinforced C-Shape Cross-Section Beam (3-Point Bending Test)



Figure 15. Design for Reinforced C-Shape Cross-Section Beam (4-Point Bending Test)